Adsorption Site and Surface Temperature Effects in CO Formation on Pt(111): A New Semiclassical Study†

M. Cacciatore,*,‡ E. Christoffersen,§ and M. Rutigliano‡

CNR−IMIP sezione di Bari, c/o Dipartimento di Chimica, Università di Bari, via Orabona N.4, 70126 Bari, Italy

Received: February 27, 2004; In Final Form: May 18, 2004

This study focuses on the dynamics of CO formation on Pt(111). To this end, a new semiempirical interaction potential was derived by using much of the most recent experimental information obtained from CO chemisorbed on the on top and bridge platinum sites. The dynamics on the adiabatic potential surface has been performed according to the semiclassical collisional method developed for molecule−surface interactions. The role played by the multiphonon excitation mechanism, the adsorption site, and the surface temperature effects on the Eley−Rideal recombination dynamics and on the energy fluxes through the platinum surface and the internal states of the formed CO molecules was studied in detail.

1. Introduction

Carbon oxidation catalyzed by metal surfaces, and here specifically platinum surfaces, is among the most widely studied systems in chemisorption. CO is an important molecule in many catalytic reactions on metals, whereas Pt is among the most interesting catalysts for oxidation reactions in the chemical industry. Despite the vast amount of work performed both experimentally[1−9] and theoretically[10−15] to point out the most important features of this heterogeneous system, CO adsorption and CO formation on metallic single crystals, considered as prototype systems in the field of surface chemisorption and surface reaction dynamics, are still a subject of investigation and discussion. The reaction for CO formation can be described according to two extreme collisional mechanisms, that is the Langmuir−Hinshelwood (L−H) mechanism and the Eley−Rideal (E−R) mechanism. According to the former mechanism, the reaction takes place between the preadsorbed C and O atoms which diffuse on the surface and then recombine to form CO in the gas phase in a specific vibro-rotational state (v,j).

The "direct" E−R mechanism is a two step process: first an oxygen (or carbon) atom is chemisorbed, then a reaction occurs between the adatom and the C atom approaching the surface from the gas-phase, hitting the surface and then eventually recombining with the previously adsorbed oxygen

$$O + Pt \rightarrow O_{ad}{*}Pt \tag{1}$$

$$O_{ad}{*}Pt + C \rightarrow CO(v,j) + Pt + \Delta E \tag{2}$$

Step (2) is the rate-determining step of the E−R mechanism.

Both the L−H and the E−R reaction mechanisms have two main dynamical features: the first aspect concerns the large recombination exothermic energy that leads to a large translational and internal energy of the formed CO molecules. This aspect, common to recombination reactions in the gas-phase, is of great relevance not only from a dynamical point of view but also for practical applications. Surface recombination reactions can be an effective source of energetically activated molecules in reactive environments of importance in various fields of technological interest, as for example classical and advanced catalysis and, more generally, in CO containing mixtures under diffusive, nonthermal equilibrium conditions. The second feature concerns the sensitivity of the reaction dynamics to both the initial state of the gas-phase atom and the initial conditions of the chemisorbed particle. As a consequence, the recombination probability, and the correlated recombination coefficient γ, is a complex function of several molecular and surface variables, among which are the following: the kinetic energy and the orientation angles of the gas-phase atom, the adsorption site of the adsorbed oxygen, the temperature of the platinum surface, and, in general, the structural and chemical properties of the surface.

It turns out that detailed collisional data, such as the vibrational state-selected recombination probability and the kinetic and internal energy distribution of the scattered CO molecules, cannot be easily measured in experimental investigations. Thus, to gain an insight into the dynamics and the energetic of CO formation, molecular dynamics studies can be of great relevance. We have therefore applied to this system the semiclassical approach developed by Billing to the gas−surface interaction dynamics. This method, which was developed at the beginning of the 80's,[16,17] and first applied to the C [12] and CO [13] oxidation on Pt(111), is able to describe the most important features of the molecule−surface interaction, including the phonon and the electron−hole excitation mechanism in the solid substrate.

The accuracy of the results obtained with this method, as well as in any collision dynamics calculation, relies mostly on the accuracy with which the interaction potential between the interacting particles is known. This is a critical point since the interaction potential in its full dimension is practically unknown for molecule−surface interactions, except for very few elemen-

† Part of the "Gert D. Billing Memorial Issue".

* To whom correspondence should be addressed. E-mail: cacciatore@area.ba.cnr.it. Fax: +39 080-5442024. Tel: +39 080-5442101.

‡ Università di Bari.

§ Post Doc position at the CNR-IMIP, Bari (Italy) and Department of Chemistry, H. C. Ørsted Institute, University of Copenhagen, DK-2100Ø Denmark.

10.1021/jp040188z CCC: $27.50
Published on Web 07/16/2004

tary systems, notably the dissociative chemisorption of H_2 on transition and noble metals.[18,19]

The revision of our previous study[12] on CO formation on a platinum surface was motivated by the great progress made in the past few years, both experimentally and theoretically, which has brought about a better characterization of the molecule/surface interaction potential and has added new accurate data and details on the properties of the chemisorbed species involved in the recombination reaction. The analysis of the new acquired data is of great relevance in the building up of a new, more realistic interaction potential and thus to improve and verify the studies and the results emerged in previous collisional works.

For the CO/Pt system, the earlier electronic structure calculations date back to the classical work of Blyholder[20] where the well-known synergism between electron donation and back-donation between the molecular orbitals of the CO molecule and the electronic d-band of the metal was proposed. Recently, density functional (DFT) calculations have been performed for atomic O and CO bonding on metallic surfaces.[21−27] A good agreement between the experimental and the calculated adsorption energy, the downshift of the vibrational frequencies and the relaxed equilibrium geometries was generally found in these ab initio studies. However, due to obvious computational time limits, ab initio calculations have been limited to specific portions of the potential energy surface (PES): fixed orientation geometry and single adsorption site, so that a complete PES for CO adsorption on Pt(111) is not yet available.

To construct an adiabatic potential surface, we therefore followed a semiempirical approach which incorporates much of the experimental data that have been available from recent experimental investigations. In particular, our primary sources were the spectroscopic data determined in He scattering experiments performed by Lahee et al. on CO chemisorbed on Pt(111).[1] As will be shown in the next sections, the newly obtained PES is different in some important aspects which, in fact, have consequences on the dynamical behaviors of the recombination reaction.

As a result of the semiclassical trajectory calculations performed on the semiempirically determined potential energy, a large mass of collisional data were obtained which concerns, primarily, the global and state-selected probability for CO formation in a specific (v,j) state, the translational and the internal energy distribution of the desorbing molecules, and the energy transferred to the surface due to the phonon excitation/de-excitation processes. Only part of the full results is shown here. Some important aspects of the catalytic reaction have been exploited. In particular, we focused on (a) adsorption site and (b) orientation angle effects, (c) the importance played by the multi-phonon excitation mechanism, and (d) the intrinsic effect of the surface temperature on the catalytic activity of the platinum surface. The effects in b−d were not studied in our previous work. Therefore, the present study may be considered a significant improvement to the previous data due to the new surface effects studied and the improved potential energy surface derived and used in the dynamics.

2. Interaction Potential

Following the previous study on this system,[11,12] the interaction potential for CO formation on platinum is expressed as a sum of pairwise C,O−Pt atom interactions with each interaction term given as a Morse-like potential with two extra terms

$$V(R,r) = \sum_{i=1}^{2}\sum_{\alpha=1}^{N} \exp(-\beta_i R_{i\alpha})[D_i \exp(-\beta_i R_{i\alpha}) - E_i + B_i R_{i\alpha} + C_i {R_{i\alpha}}^2] + D_{CO}[1 - \exp(-\beta(r - r_{eq}))]^2 \quad (3)$$

where $R_{i\alpha}$ is the distance between atom i in the gas-phase and the atom α of the platinum surface. r and r_{eq} are the C−O distance and the equilibrium CO bond distance, respectively, and N is the total number of the lattice atoms. In the above equation, there are five parameters for each pair interaction (C and O in CO interacting with a Pt surface atom) to be determined.

The interaction for the isolated C and O atoms with the platinum surface are described in the same way but using pure Morse functions.[11,12]

To get the correct asymptotic behavior of the reactive PES, the parameters in the eq 3 are switched in the dissociation limit to the C−Pt and O−Pt interaction potential. Thus, we have

$$\beta_i = b_i f_1 + bb_i(1 - f_1) \quad (4)$$

$$D_i = d_i f_1 + dd_i(1 - f_1) \quad (5)$$

$$E_i = e_i f_1 + ee_i(1 - f_1) \quad (6)$$

$$B_i = h_i f_2 \quad (7)$$

$$C_i = k_i f_2 \quad (8)$$

where the two switching functions f_1 and f_2 are given as

$$f_1 = \exp[-a_1(r_i - r_{eq})^2] \quad (9)$$

$$f_2 = \exp[-a_2(r_i - r_{eq})^2] \quad (10)$$

According to the proposed damping functions, the set of parameters (bb_i, dd_i ee_i) defines the interaction of the isolated carbon and oxygen atom with the platinum surface, whereas the parameters (b_i, d_i, e_i, h_i, k_i) correspond to the interaction of C (in CO) and O (in CO) with the platinum surface.

With the assumed potential, a normal-mode analysis for the CO chemisorbed on Pt(111) has been followed for the adsorption site configurations to which the corresponding normal-mode frequencies are known. The potential parameters are then determined by a nonlinear optimization procedure such that a satisfactory agreement between the calculated and the reference experimental frequencies and the chemisorption energies is reached. Our primary source for the experimental data is the investigation made by Lahee et al.[1] where the high frequencies as well as the low frequencies of the vibrational normal modes for chemisorbed CO in the on top and bridge sites were determined. The relaxed geometries for these two sites, which bind CO to the Pt(111) surface under thermal equilibrium conditions, are shown in Figure 1. The assumed equilibrium geometries, taken from ref 3, are in good agreement with DFT calculations.[24−26] The C_{6v} symmetry for the on top configuration leads to four nondegenerate normal modes corresponding to the intramolecular (C−O) and the intermolecular (CO)−Pt stretching frequencies, whereas the two remaining doubly degenerate low-frequency modes correspond to the hindered rotations and hindered translation both parallel to the surface. The C_{4v} cluster symmetry for the bridge site leads to six nondegenerate normal modes.

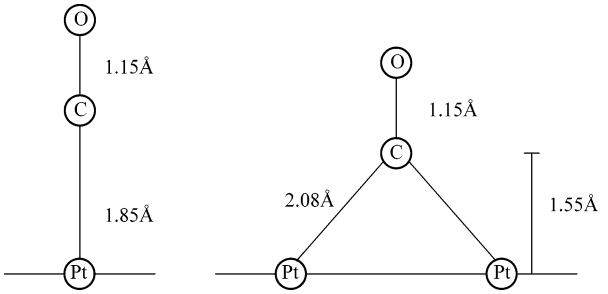

Figure 1. CO adsorbed in the on top and bridge site. Positions taken from ref 3.

TABLE 1: Experimental and Theoretical (Second Line in Italics) Normal Mode Frequencies of CO Chemisorbed on the Bridge and the On Top Site of Pt(111)[a]

on top	ω_1	ω_2	ω_3	ω_4		V_0
expt	2084[b]	469[d]	387[c]	48.5[c]		−1.36[f]
theory	*2063*	*451*	*307*	*64*		*−1.40*
bridge	ω_1	ω_3	ω_2	ω_5	ω_4	ω_6	
expt	1850[b,c]	425[c]	380[c]	350[e]	141[c]	60[b]	−1.14[f]
theory	*2007*	*319*	*261*	*178*	*88*	*185i*	*−0.97*

[a] The frequencies are in units of cm^{-1}. The binding energies V_0 are in eV. [b] Reference 6. [c] Reference 1. [d] Reference 5. [e] Reference 4. [f] Reference 2.

The appropriate normal-mode frequencies can be obtained by solving the secular equation of the force constants matrix

$$|\bar{H} - \bar{E}\lambda| = \bar{0} \tag{11}$$

where $\bar{E}$ is the unitary matrix and λ is the diagonal matrix of the normal-mode frequencies. $\bar{H}$ is the dynamical matrix of the force constants

$$H_{ij} = \frac{1}{\sqrt{m_i m_j}} \frac{\partial^2 V}{\partial R_{i\alpha} \partial R_{j\beta}} \tag{12}$$

where V is the CO−Pt interaction potential given by eq 3 and m_i is the mass of atom i.

The $\bar{H}$ matrix is diagonalized numerically, and the obtained eigenvalues are compared with the reference experimental values. The potential parameters are determined by the minimization of the function S

$$S = (V_T(\bar{x}) - V_T^e)^2 + (V_B(\bar{x}) - V_B^e)^2 + \left(\frac{\partial V}{\partial z}\Big|_T\right)^2 + \left(\frac{\partial V}{\partial z}\Big|_B\right)^2 + \sum_{k_T}^{6}(\omega_{k_T}(\bar{x}) - \omega_{k_T}^e)^2 + \sum_{k_B}^{6}(\omega_{k_B}(\bar{x}) - \omega_{k_B}^e)^2 \tag{13}$$

defined such that each term represents the quadratic standard deviation between the calculated and the experimental spectroscopic constants. In the above equation, $\bar{x}$ is the vector of the potential parameters, ω_{k_T} is the calculated frequency of the kth normal mode in the on top site, and $\omega_{k_T}^e$ is the corresponding experimental value. V_T is the binding energy for the on top configuration. The subscript B denotes the bridge site. The function S was minimized to the value 0.0032 eV^2.

The result of the diagonalization-plus-minimization cycles is shown in Table 1 where the spectroscopic data obtained from various sources and the data calculated from our best-fitted interaction potential are reported. We note that the frequencies, as well as the chemisorption energies, are quite well reproduced. However, we were unable, with the assumed functional form of the potential, to reproduce the lowest ω_6 frequency for the bridge site (an imaginary value, 185i, was obtained for this frequency). This frequency, although important for the surface diffusion process, as for example the L−H recombination mechanism, is less relevant for the "direct" recombination process here considered.

TABLE 2: Potential Parameters for CO/Pt(111) Interaction Given by Equations 3−10 Obtained from the Optimization-minimization Procedure (Energy in eV)

	C in CO $i=1$	O in CO $i=2$		C $i=1$	O $i=2$
b_i	3.83$Å^{-1}$	1.75 $Å^{-1}$	bb_i[a]	2.016 $Å^{-1}$	2.21 $Å^{-1}$
d_i	1.02×10^6	209.4.	dd_i[a]	3386.0	13303.7
e_i	1212.6	−168.9	ee_i[a]	150.0	245.2
h_i	−605.3	132.7			
k_i	−77.9	−46.1			

$a_1 = 2.32$; $a_2 = 2.00$;
CO Morse parameters:[b] $D_{CO} = 10.826$ eV; $r_{eq} = 1.128$; $\beta = 2.34$ $Å^{-1}$

[a] Taken from ref 11. [b] Reference 28.

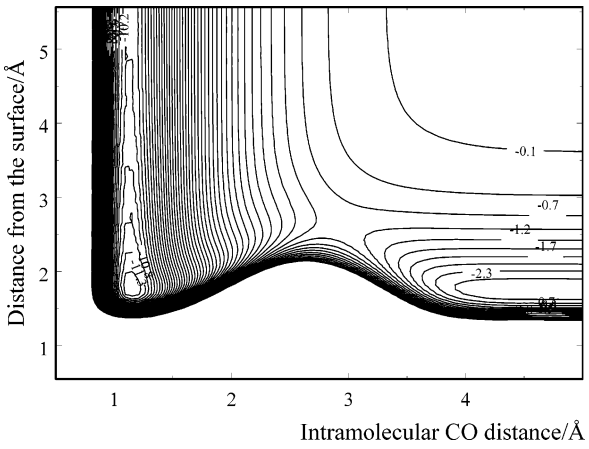

Figure 2. Contour plot of the semiempirical potential energy surface of CO interacting in the perpendicular geometry on the on top Pt(111) site. The potential is reported as a function of the normal distance of the C atom to the surface and the C−O bond distance. Energies are in units of ϵ, $1\ \epsilon = 1.03640$ eV.

The result of the best fit potential parameters is given in Table 2.

The interaction potential obtained with this approach can be considered reliable enough in that the semiempirical potential is able to well reproduce the most recent spectroscopic data of the chemisorbed species. Figure 2 shows the contour plot of the interaction potential for CO in the perpendicular geometry interacting in the on top Pt(111) site. The potential is reported as a function of the intramolecular C−O distance and the distance of the C atom from the first surface layer. The potential is defined as $V = V_{C,O,CO-Pt} + V_{CO}$, where V_{CO} is the intramolecular Morse potential of CO (the corresponding Morse constants are taken from ref 28). The geometry and the binding energy of CO in the chemisorption well are very close to the experimental values[2,3] reported in Figure 1 and in Table 1. In this configuration the PES exhibits a barrier for the CO formation of 1.5 eV.

With regards to the potential obtained in refs 11 and 12, it is worthwhile noting that the new potential here calculated is based on larger and updated data. Important differences emerge by comparing the two potential surfaces. In particular, in ref 11, the equilibrium distance of CO from the platinum surface was set to 2 Å in both the bridge and the on top geometries. This value is much larger than the experimental distances obtained in later works[2,3] but assumed in the present study (see again

Figure 1 for the on top perpendicular interaction). Furthermore, in the previous potential, the CO molecule adsorbed in the perpendicular configuration at distances from the surface shorter than 1.2 Å exhibits a C−O bond distance close to 2 Å (Figure 4 of ref 11): such a stretched bond distance does not appear realistic, and it is definitely too large compared to the bond distances of CO chemisorbed in the equilibrium configurations (see Figures 1 and 2). Moreover, a further source of improvements concerns the normal-mode analysis conducted in the present work which includes all of the six frequencies, associated with the on top and bridge adsorption geometries, determined in the diffraction experiments. In our previous study, only the two higher frequencies were considered in the potential energy derivation.

On the basis of these arguments, the newly calculated interaction potential can be considered more accurate and physically acceptable. In addition, the improvements made on the PES have, as will be shown in section 4, a large impact on the surface dynamics.

3. Semiclassical Collisional Method

To simulate the nuclear motion of the gas-phase particles, C and O atoms, over the calculates PES the semiclassical collisional method has been followed. This method has been applied to describe the dynamics of the dissociative chemisorption of H_2, N_2, CO, and other diatomic molecules on metals, semiconductors, and oxide surfaces.[29−33] Recently, it has been extended to larger molecules and clusters in the more complex classical-quantum formulation.[34] The semiclassical method is given in a number of papers[16,17,35] and is fully described in ref 36, so that only the essential is reported here.

The method is semiclassical in the sense that the dynamics of the phonons is treated quantum-mechanically while the motion of gas-phase species is treated classically by solving the relevant Hamilton equations of motion. The coupling between the classical degrees of freedom and the surface phonons is made via a time and surface temperature-dependent effective potential H_{eff} of the mean-field type. Thus, we have

$$H_{\mathrm{eff}} = \frac{1}{2}\sum_{i,\gamma}\frac{1}{m_i}P^2_{i,\gamma} + V_{\mathrm{CO}}(r_{\mathrm{C-O}}) + \Delta E_{\mathrm{ph}} + V_{\mathrm{add}} \quad (14)$$

where the first term is the classical Hamiltonian of a diatom interacting with the surface, $P_{i\gamma}$ is the γth Cartesian component of the momentum of atom i having mass m_i, $V_{CO}(r_{C-O})$ is the intramolecular potential of the free molecule, and ΔE_{ph} is the energy exchanged with the surface phonons. In eq 14, V_{add} is the additional term given as the expectation value of the interaction potential over the phonon wave function

$$V_{\mathrm{add}}(t,T_{\mathrm{S}}) = \langle \Psi(t,T_{\mathrm{S}})|V_{\mathrm{int}}|\Psi(t,T_{\mathrm{S}})\rangle \quad (15)$$

where t is the interaction time, V_{int} is the interaction potential between the gas species and the surface atoms, and $\Psi(t,T_S)$ is the total wave function of the phonon modes given as a distribution of quantum states at a fixed surface temperature T_S

$$\Psi(t_0) = \sum p_{\{n_0\}}(T_S)^{1/2}|\{n_0\}\rangle \quad (16)$$

$p_{\{n_0\}}$ is the Boltzmann energy distribution for a given T_S. The time evolution of the phonon wave function can be obtained by solving analytically the time-dependent Schrödinger equations of motion under the harmonic oscillator approximation, that is assuming that a set of $M = 3N - 6$ (N is the number of atom in the considered 3D lattice) independent harmonic oscillators are perturbed by the linear (and quadratic) forces exerted between the atom/molecule approaching the surface from the gas-phase and the solid substrate. Thus, by expanding the interaction potential in the normal mode coordinates, the following dynamical Hamiltonian is obtained:

$$V_{\mathrm{add}} = V_0 + \sum_i V_k^{(1)}\eta_k(t) \quad (17)$$

where V_0 is the "static" interaction potential between the atoms in the gas-phase and the lattice atoms in their equilibrium positions. $V_k^{(1)} = \partial V_{\mathrm{int}}/\partial Q_k|_{\mathrm{eq}}$ is the linear driving force exerted on each kth phonon mode Q_k. $\eta_k(t)$ are the "phonon excitation strengths" given in terms of the Fourier components $I_{i,k}(t)$ of the external force

$$\eta_k(t) = -\int \mathrm{d}t'(\hbar\omega_k)^{-1}\frac{\mathrm{d}}{\mathrm{d}\rho_k}(\Delta E_k^+ + \Delta E_k^-)\,[I_{c,k}(t')\cos(\Theta_k(t',\omega_k)) + I_{s,k}(t')\sin(\Theta_k(t',\omega_k))] \quad (18)$$

$$I_{c,k} = \int_{-\infty}^{+\infty}\mathrm{d}t\, V_k^{(1)}(R(t))\cos(\omega_k t) \quad (19)$$

with $\Theta_k(t, \omega_k) \approx \omega_k t$, ω_k being the frequency of the kth phonon mode.

$\Delta E_k^{\pm} = \Delta E_k^{\pm}(\omega_k, \rho_k^{\pm}; T_S)$ is the energy exchanged between the chemical particles in the gas-phase and the solid substrate due to the phonon creation (ΔE_k^+) and phonon annihilation (ΔE_k^-) processes of m vibrational quanta in the kth phonon mode.

The phonon eigenvectors and the phonon frequencies are obtained by a numerically diagonalizing the 3D dynamical matrix of the force exerted between the nearest and second-nearest neighbor platinum atoms according to the procedure followed in the previous work.[11] The Pt(111) surface sample assumed in the phonon dynamics and in the scattering calculations consists of a 3D lattice with 35 and 30 Pt atoms disposed on the first and second layer, respectively, according to the (111) crystallographic geometry.

4. Results and Discussion

In the dynamics simulation, we assume that the O atom is adsorbed in a specific surface site in thermal equilibrium with the surface temperature, whereas the initial position coordinates of the gas phase carbon atom are picked randomly in an aiming area equal to the Pt(111) unit cell area. The impact energy of the impinging C atom was fixed to $E_{coll} = 0.5$, 1, 2, and 3 eV. In the orthogonal frame of reference, the topmost Pt layer lies on the (X,Y) plane, the Z axis being the normal axis. The incident orientation angles are (θ, φ), where θ is the angle between the position vector of the C atom and the Z axis, φ is the corresponding azimuth angle. A number of about 700 trajectories were calculated for each impact energy considered in the simulation.

In Figure 3, the semiclassical recombination probability is reported as a function of the impact energy of the carbon atom. Two cases were considered: the oxygen can be adsorbed on top or on the bridge site. We note that there is a large site specific effect in the CO formation, the recombination probability for the bridge site can be up to four times larger than the probability for the on top site. This is mainly a consequence of the different recombination mechanism activated in the two lattice sites. The detailed analysis of the reactive trajectories reveals that the recombination reaction is in competition with the adsorption of the C atom at the surface. In other words, the

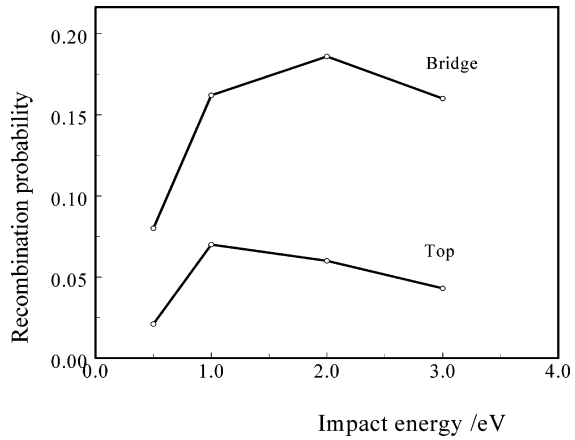

Figure 3. Semiclassical recombination probability for the E−R reaction: C + O_{ad}*Pt(111) → CO + Pt(111). The oxygen atom is chemisorbed in the on top and bridge site. The gas-phase atom hits the surface with E_{coll} = 0.5, 1, 2, and 3 eV. The incident angles (θ,φ) are set equal to (45,0)°, T_S = 300 K.

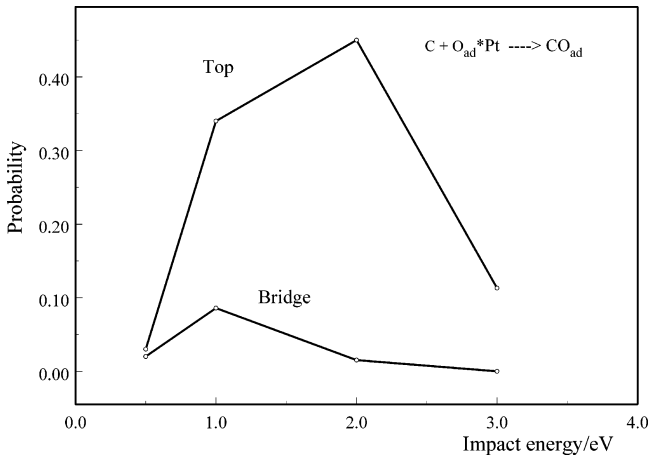

Figure 4. Probability for CO formation and adsorption in the reaction: C + O_{ad}*Pt(111) → CO_{ad}*Pt(111). The initial scattering conditions are the same as for Figure 3.

adsorption of the carbon atom prevents the CO formation at the surface, so that the most favorable condition for CO formation occurs when the adsorbed oxygen is scattered from the surface so as to screen the surface from the incoming gas-phase carbon atom. This screening effect, which was pointed out also in our previous study,[12] is effective in two cases: (a) when the oxygen is scattered from the surface into the direction of the incoming C atom and (b) when the O atom sits on the surface for a time large enough to react with the C atom. Both these effects are site-dependent. The chemisorption energy of the oxygen atom on the bridge site is larger than that for the on top site (E_{ad} = 3.5 and 2.8 eV, respectively) so that the oxygen atom remains bounded on the surface in the bridge site, or in its environs, for a longer time.

The probability for CO adsorption at the platinum surface is much larger when the oxygen atom is adsorbed on the on-top site compared with the probability obtained when the oxygen sits on the bridge site. This can be seen from the results reported in Figure 4 where the probability for the process

$$C + O_{ad}*Pt \rightarrow CO_{ad}*Pt \qquad (20)$$

is reported as a function of the impact energy. The behavior shown in Figure 4 is due to the binding energy of CO which is larger in the on top site. Although the semiclassical trajectories

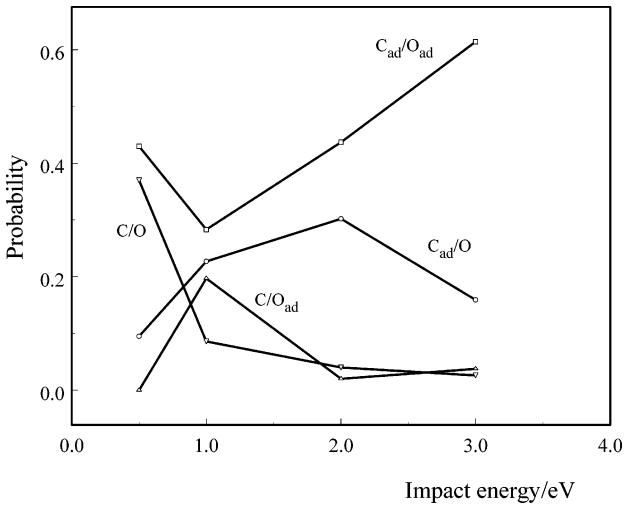

Figure 5. Probabilities as a function of the impact energy for C and O atom reflection, adsorption and adsorption/desorption processes in the reaction: C + O_{ad}*Pt(111) → "products" + Pt(111). O_{ad} is initially adsorbed in the bridge site, T_S = 300 K.

are numerically very stable, the analysis of the adsorption collisions requires some caution. Typically, the motion of the adsorbed CO molecules takes place at distances from the surface layer less than 2.3 Å and cannot be followed for times longer than 3−4 picoseconds. At longer collision times, the CO molecule propagates at a distance from the surface smaller than 0.9 Å, so that the coupling with the phonons becomes much stronger and the trajectory unstable. As a consequence, the migration of the adsorbed species on the surface cannot be followed on a longer time scale. It is worth noting that, according to the criterion adopted, the adsorption processes occur for the stable trajectories when the available escape energy, $H_{eff} - \Delta E_{ph} - E_{vib}^{(0)}$, $E_{vib}^{(0)}$ being the zero point energy of the adsorbed species, is much less than the adsorption energy, $V_{add} + V_0$.

In addition to the CO formation in the gas-phase (2) and CO formation at the surface (20), the interaction of the C and the O atom with the platinum surface can lead to the activation of several other processes in competition with one another, among which:

(1) Direct inelastic scattering where both atoms are reflected into the gas-phase after one or two bounces on the surface.

(2) Adsorption/desorption processes where at least one of the two atoms is scattered in the gas-phase, or when CO is temporarily adsorbed on the surface in a specific (v′,j′) state before desorbing as CO(v,j). It turns out that this latest mechanism for the CO formation can be effective and in close competition with the "direct" CO formation, particularly when CO is formed near the platinum surface.

(3) Finally the adsorption, or sticking, processes. In this case, both the C and the O atom, or the eventually formed CO, remain bound to the surface.

Due to the concurrency of such different physicochemical effects, the dynamics of the processes taking place at the surface can be very complex.

Figure 5 shows the calculated probabilities of the various adsorption and adsorption/desorption processes in the reaction: C + O_{ad}*Pt(111) → "products", and O_{ad} chemisorbed on the bridge site. We note that, in the full energy range, the most effective processes are those where both the C and the O atoms are adsorbed at the surface (C_{ad}/O_{ad}). This adsorption channel is in close competition and correlated with the process where the carbon atom is adsorbed and the O desorbs in the gas-phase. At the higher impact energies, the probability for the carbon

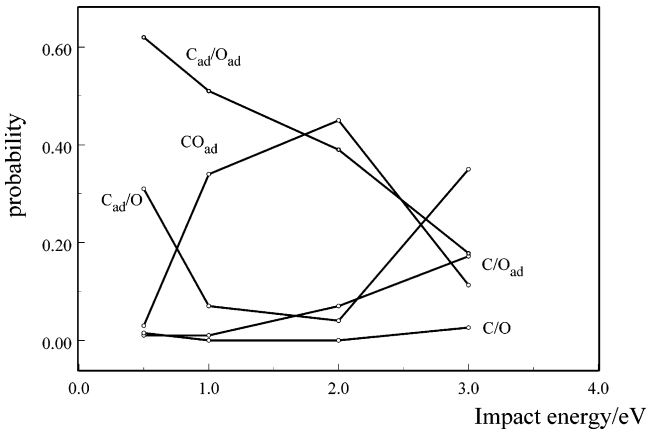

Figure 6. Same as in Figure 5 but O_{ad} is adsorbed in the on top platinum site.

atom to be scattered from the surface is smaller than the probability for the oxygen to desorb and this is a consequence of the different binding energies.

The dynamics of the surface processes is different when the oxygen atom is chemisorbed on the top site. This can be readily seen by comparing the results of Figure 5 with the probabilities reported in Figure 6 for the top site case. In this latter case, the dynamics at the surface is much more involved due to the more effective competition between the various inelastic and reactive adsorption and adsorption/desorption processes. In particular, we note the strict correlation between the CO adsorption processes and the processes where the carbon atom is adsorbed and the oxygen scattered in the gas phase. At the highest impact energy, the carbon atom is adsorbed preferentially thus preventing the CO formation.

Furthermore, a cross comparison between the recombination probabilities reported in Figure 3 for O on the top Pt site and the probabilities of the inelastic processes of Figure 6 reveals some interesting correlation effects among the various processes going on at the surface. At the lowest impact energy, $E_{coll} = 0.5$ eV, the close interplay between the CO formation reaction and the two, much more effective adsorption processes, C_{ad}/O_{ad} and C_{ad}/O, is well evident. On the other hand, the decreasing of these two adsorption processes, not compensated by the fast increase of the probability for CO adsorption, is responsible for the observed increasing recombination probability as the impact energy increases to 1.eV. At the two higher energies, $E_{coll} = 2-3$ eV, the opening of the two other inelastic channels for C/O and C/O_{ad} formation is responsible for the slight decrease of the CO formation in the gas-phase.

Comparison between the new collisional data and the precedent results[12] can be made for O_{ad} in the on-top site only, since the bridge site (slightly more stable) was not considered in ref 12. Inspection of the data reported in Table 3A,B) shows that the dynamics and the energetic on the two potential surfaces are quite different both from the qualitative and the quantitative point of view. We note that, for O adsorbed on the on top site, the new potential energy surface is less reactive than the previous one, the new recombination probability being a factor of 3 smaller at $E_{coll} = 1$ eV. At $E_{coll} = 2$ and 4 eV the newly calculated recombination probabilities are $P_r = 0.055$ and 0.043, respectively, whereas the values obtained with the old potential were $P_r = 0.11$ and 0.12, respectively. On the other hand, we now have a much larger sticking probability (CO adsorbed as a molecule and as isolated atoms), particularly at the two lowest impact energies. As far as the energetic of the recombination reaction is concerned, a comparison between the new and the previously obtained results can be made on the basis of the data of Table 3B). Here, the energy transferred to the platinum surface and the average rotational and vibrational quantum numbers of the formed CO molecules are reported. Compared to the previous study, the energy interplay between the surface phonons and the internal motions of CO behaves differently, as well as its variation with the collisional energy. In particular, the lowest phonon excitation, and the consequently largest roto-vibrational excitation in CO, now occurs at $E_{coll} = 3$ eV, whereas at this collisional energy, the energy exchanged with the phonon was maximum with the previous interaction potential.

TABLE 3: (A) Product Probabilities in the Reaction C + O_{ad}*Pt(111) → "products"[a] and (B) Average Vibrational and Rotational Actions of CO in ħ units, ⟨*n*⟩ and ⟨*j*⟩ Respectively, Reported for the Reactive Collisions, Together with the Average Energy Transferred to the Pt Surface Phonons, ⟨ΔE_{ph}⟩[b]

(A) "Products" Channel Probabilities

E_{coll}/eV	$C_{ad} + O$	$C + O_{ad}$	$O_{ad} + C_{ad}$	C + O	CO_{ad}[c]	CO
1.0	0.07(0.3)	0.01(0.04)	0.51(0.36)	0.0(0.0)	0.34	0.07(0.28)
2.0	0.04(0.19)	0.07(0.09)	0.39(0.61)	0.0(0.0)	0.45	0.05(0.11)
3.0	0.37(0.26)	0.19(0.08)	0.20(0.46)	0.087(0.08)	0.11	0.043(0.12)

(B) Reactive Collisions: CO

E_{coll}/eV	⟨*j*⟩/ħ	⟨*n*⟩/ħ	⟨ΔE_{ph}⟩/10^4 K
1.0	85(78)	17(22)	2.37(2.90)
2.0	112(123)	16(20)	4.21(2.29)
3.0	150(84)	23(14)	2.36(5.52)

[a] In the initial conditions O_{ad} is adsorbed on the on top site, $T_S = 300$ K, $(\theta,\varphi) = (45,0)°$. The numbers in parenthesis are the results of ref 12. [b] The initial conditions are the same as in Table 3a. The numbers in parentheses are from ref 12. [c] Molecular adsorption was not checked in ref 12.

The large differences pointed out in this analysis are primarily due to the changes of the new interaction potential. The dependence of the phonon coupling upon the interaction potential is formally rather involved,[35] so that the effects observed on the energy exchange mechanism, and, as a consequence, on the surface dynamics, due to the interaction potential modifications cannot be easily predictable.

However, the obtained results can be considered a further demonstration of the sensitivity of the surface process dynamics upon the details of the interaction potential (in the region of the chemisorption wells) and, therefore, of the necessity for searching a PES as much accurate as possible.

The dynamics of the surface processes is controlled by different factors. The energy exchange mechanism between the platinum surface (phonons and/or electrons) and the interacting particles plays a role on the surface dynamics overall and, more specifically, on the adsorption/desorption processes. In the semiclassical model, the phonon excitation/de-excitation processes are included in the collision dynamics through the "dynamical" Hamiltonian V_{add}, so that the effect of this coupling mechanism between C, O, CO, and the surface phonons can be evaluated. The effect of the electron−hole excitation was studied for the dissociative chemisorption of H_2/D_2 on Cu(111).[29]

The energy partitioning of the exothermic energy released in the recombination reaction at $E_{coll} = 0.5$ eV is shown in the upper part of Table 4 where the energy fraction transferred to the kinetic and the roto-vibrational motions of the formed CO molecules and to the surface phonons has been reported.

To point out the adsorption site effect on the energy transfer mechanism, two different sites for the adsorbed oxygen atom,

TABLE 4: Adsorption Site and Orientation Angle Effect on the Energy Flow Pathway in the Reaction C + O_{ad}*Pt(111) → CO(v,j) + Pt(111)[a]

adsorption site	E_{vib}	E_{rot}	E_{kin}	ΔE_{ph}
	E_{coll} = 0.5 eV, (θ, φ) = (45°,0)			
top	25.52	32.34	19.61	22.60
bridge	45.04	24.78	7.13	23.25
	E_{coll} = 1.0 eV, Bridge Site			
angles (θ, φ)°				
(0,0)	47.67	21.35	16.38	14.60
(45,0)	46.20	16.10	15.92	21.75

[a] E_{vib}, E_{rot}, and E_{kin} are the energy fraction (%) transferred to the vibrational, rotational, and translational motion of CO, respectively. ΔE_{ph} is the energy fraction transferred to the surface phonons. The surface temperature is T_S = 300 K.

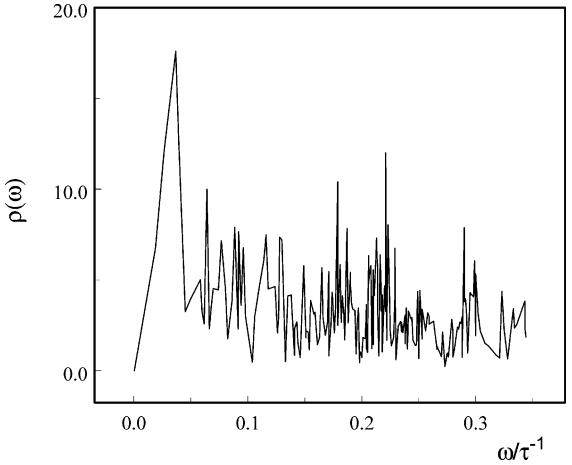

Figure 7. Excitation strength ρ_k for the phonon modes of Pt(111) K35/30 for a specific recombination collision taking place at the surface. (E_{coll} = 2 eV and O_{ad} in the bridge site.) The frequencies are in τ^{-1} units, 1 cm^{-1} = 1.88364 × 10^{-3} τ^{-1}.

the bridge and the on top site, were considered in two different simulations. The energy transferred to the surface is, in both cases, not negligible since up to about 25% of the reaction exothermic energy goes into the phonon states (for the adsorption processes, the phonon excitation is much more effective).

The results in Table 4 show that the adsorption site has a large impact on the energy partitioning in CO, particularly for the energy interplay between the roto-vibrational motions of the formed molecules. The energy transferred to the surface does not change significantly, at least for the initial conditions considered.

To gain insight into the phonon excitation mechanism in reactive collisions, in Figure 7 we have reported the phonon excitation strengths, $\rho_k(t,T_S)$, as a function of the phonon normal-mode frequency ω_k calculated for a typical reactive collision: C + O_{ad}*Pt(111) → CO(v = 15, j = 94), at E_{coll}= 2 eV and O_{ad} placed on the bridge surface site. The reported ρ_k were monitored at the collision time where CO is formed.

From the reported spectrum, two considerations can be pointed out: first, the most excited modes are, as expected, the high energy phonon modes, although the optical modes can be excited at the higher impact energies. The second consideration concerns the number of vibrational quanta involved in the excitation mechanism. The number of phonons $\langle m_k \rangle$ that can be excited or de-excited in the kth normal mode due to the molecule-surface interaction is correlated to the ρ_k (see ref 17 for details).

Therefore, from the calculated excitation strengths, it can be observed that a multi-phonon excitation mechanism is active

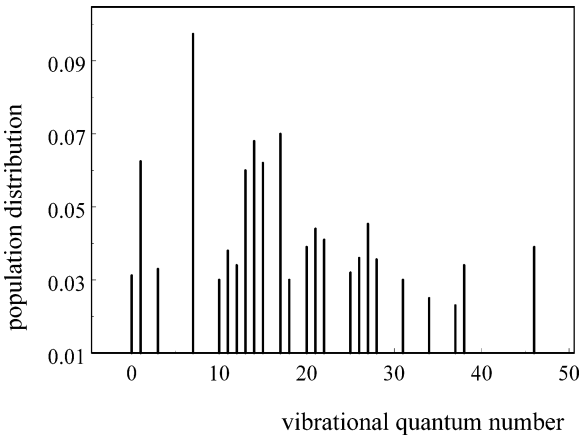

Figure 8. Vibrational distribution function of CO formed in the reaction: C + O_{ad}*Pt(111) → CO + Pt(111). O_{ad} is in the bridge site, T_S = 300 K, E_{coll} = 1 eV, (θ,φ) = (45,0)°.

in the recombination reaction in that several quanta, about 10−15, can be involved in the energy transfer dynamics. This aspect is among the most basic features of the molecule−surface dynamics, and the results obtained within the semiclassical method demonstrate the necessity to go beyond single-phonon excitation models. It is worth mentioning that the validity of the energy exchange mechanism treated according to the semiclassical method was assessed in a combined experimental and theoretical study on Xe scattered from GaSe(001).[37] In this work, an excellent agreement was found between the distributions, in energy and angles, of the scattered Xe atoms measured in molecular beam experiments and the corresponding distributions calculated with the semiclassical method.

In the present study, the influence of the incident angles on the dynamics was also explored.

Contrary to the adsorption site, the impact angle θ of the gas-phase atom has large consequences also on ΔE_{ph}. This can be seen from the data obtained in two test cases, where it was assumed that the gas-phase atom hits the surface with two different orientation angles, (θ, φ) = (0,0) and (θ, φ) = (45,0) respectively, while the oxygen atom is chemisorbed on the bridge site. In both cases the collisional energy is E_{coll} = 1 eV. At this impact energy, the probability for CO formation is slightly larger at normal incidence, P_r = 0.18 and P_r = 0.14 for the incidence θ = 0 and θ = 45, respectively. The orientation angle effect on the energy partitioning for the two considered orientations is reported in the lower panel of Table 4. We note that for the head-on collisions the rotational excitation is higher, whereas the phonon excitation energy is smaller due to the shorter residence time observed for these collisional events.

For the considered scattering conditions, the most consistent fraction of the reaction exothermicity is generally transferred into the vibrational motion of CO. A typical CO vibrational distribution is shown in Figure 8 for O_{ad} in the bridge site and E_{coll} = 1.0 eV. The obtained distribution shows that the full vibrational spectrum can be excited, although the low and medium-lying vibrational states are the most excited ones. The distribution peaks at v = 6 with $P_r(v = 6)$ = 0.098. For the top site case, not reported here, the corresponding vibrational distribution exhibits a peak at v = 11, with a population probability $P_r(v = 11)$ = 0.23.

An important issue in molecule−surface interactions is the influence of the surface temperature on the dynamics, an effect which is not easily predictable due to the correlation of the surface temperature effect with different factors at micro and macroscopic levels: mobility of the adsorbed surface species,

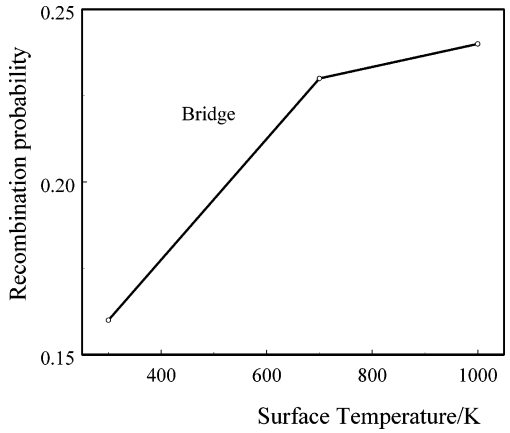

Figure 9. Semiclassical recombination probability for CO formation in the E−R reaction on Pt(111) calculated at three different surface temperatures: $T_S = 300$, 700, and 1000 K. O_{ad} is adsorbed in the bridge site, the impact energy is $E_{coll} = 1$ eV.

surface coverage, and structural modifications due to thermal and chemical effects. In addition to this, both the reaction mechanism (whether "direct" or "indirect" via a long-lived adsorbed molecular complex) and the energy exchange mechanism can also play a key role in the surface temperature effect. A surface temperature effect is generally expected for precursor mediated surface phenomena and for surface processes where the phonon coupling mechanism prevails over the electron excitation mechanism.

To gain an insight into this aspect of great importance in heterogeneous catalysis, the development and use of a collisional model which accounts for the phonon exchange mechanism can be of some relevance. Therefore, the "intrinsic" surface temperature effect was explored for the CO formation on platinum. The probability for CO formation at three different surface temperatures is reported in Figure 9. As expected due to the direct E−R mechanism followed in the recombination reaction, the surface temperature effect is small: CO is, in fact, generally formed at distances from the surface larger than 2 Å with a weak phonon coupling. However, an increase (about a factor two) of the reaction probability is observed as the surface temperature increases from 300 to 1000 K. This is due to the changing of the phonon excitation mechanism. In fact, the energy loss to the surface decreases slightly as the surface temperature increases: as a consequence, the probability for the C atom to be adsorbed becomes smaller, whereas the mobility of the adsorbed oxygen increases and, in turn, the screening effect becomes more effective.

The effect of the surface temperature on the energy partitioning is shown in Figure 10 where ΔE_{ph} is reported as a function of the collision time for a collision having the same initial conditions ($(\theta, \varphi) = (45,0)°$; $E_{coll} = 1$ eV; O_{ad} on the bridge site) but relaxed on the platinum surface at two different temperatures, $T_S = 300$ and 1000 K. The sharp increase of ΔE_{ph} takes place when the carbon and the oxygen atoms recombine and the exothermic energy is released to the system. We note that at $T_S = 1000$ K ΔE_{ph} is two times smaller than the energy exchanged at the lower surface temperature: for this specific reactive event, the surface temperature has a large impact.

Because of this, we expect a larger internal excitation of the CO molecule formed at $T_S = 1000$ K. This is confirmed in Figure 11 where the vibrational action of CO is reported as a function of the collision time for the same trajectory shown in Figure 10. In the asymptotic region, when the CO is propagating

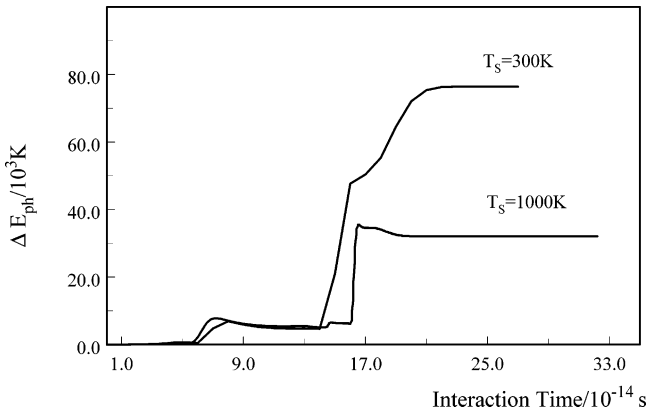

Figure 10. Energy transferred to the surface phonons, ΔE_{ph}, in the reaction: $C + O_{ad}$*Pt(111) → CO(v,j) + Pt(111). O_{ad} reported for two reactive collisions as a function of the collision time. The trajectories were run assuming the same initial conditions (see text) but relaxed on the platinum surface at two different surface temperatures T_S.

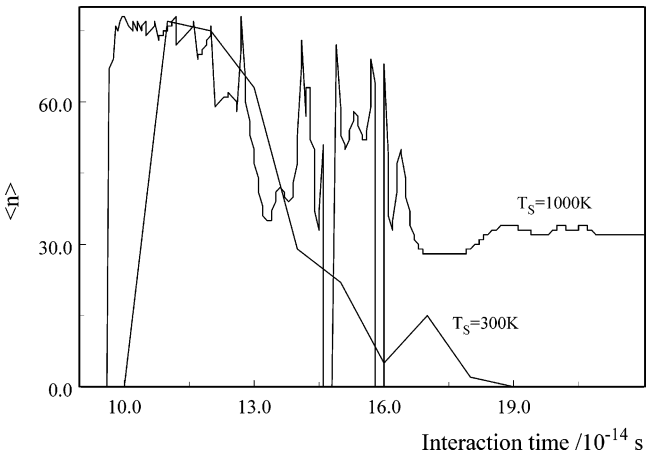

Figure 11. Classical vibrational action of the CO molecule formed in the two trajectories considered in Figure 10, shown as a function of the collision time. $\langle n \rangle$ is in units of $\hbar$.

in the gas-phase far from the surface, our results show that $\langle n \rangle = 30$ at $T_S = 1000$ K and $\langle n \rangle = 0$ at $T_S = 300$ K.

On average, the statistical surface temperature effect on the reaction energetic does not change significantly. The average $\langle \Delta E_{ph} \rangle$ fraction (% of the total energy) is 21.0, 17.3, and 17.7 at $T_S = 300$, 700, and 1000 K, respectively ($E_{coll} = 1$ eV, $(\theta,\varphi) = (0,0)°$, O_{ad} in the bridge site). Symmetrically, the kinetic and the vibrational energy of the scattered CO molecules increase slightly with the increasing of the surface temperature.

5. Final Remarks

Some basic dynamical aspects relevant to the carbon oxidation catalyzed by Pt(111) via the direct reaction mechanism have been explored using a semiempirical PES derived from the spectroscopic constants of the chemisorption species recently determined in experimental observations. Compared to the previously derived interaction potential, the new PES is different in some important aspects which have an impact on the oxidation reaction dynamics. The potentialities of the semiclassical approach to molecule−surface interaction have been exploited to study the overall dynamics of the various processes going on at the platinum surface. The obtained results show that the surface dynamics is quite complex, due to the activation of several adsorbed/desorption and sticking processes that can compete with the CO formation in the gas-phase.

The multi-phonon character of the excitation-deexcitation mechanism and the role played by this mechanism on the adsorption−desorption surface processes and on the energy flow has been pointed out. In particular, it has been found that, at least for the kinematics conditions considered in the simulation, the energy distributions of the CO molecules formed at the surface and scattered in the gas phase are correlated to the adsorption site of the adatom and to the orientation of the incoming gas-phase atom. Both effects can have an impact on the surface reaction dynamics, and they could have some consequences in the catalytic behavior of CO containing heterogeneous mixtures. The results and the effects presented in this study can be considered only on a qualitative ground, due to both the semiempirical nature of the interaction potential and the lack of experimental results for a direct comparison with the investigated effects. From this point of view, the potential energy surface obtained in this work allowed for important qualitative considerations on the phenomena underlying the surface processes.

However, some basic effects have been neglected, as for example the electron excitation processes in the substrate and the nonadiabatic character that the electronic system may exhibit in the interaction potential. As demonstrated in the study of other heterogeneous systems, these effects can be dealt with the semiclassical approach, provided that sufficient ab initio data are available for the definition and calculation of the corresponding additional terms in the effective Hamiltonian.

Acknowledgment. This work was inspired by and performed in collaboration with Prof. Gert D. Billing. One of the authors, M.C., expresses his gratitude to Gert Billing for the long years of scientific collaboration and for having had the privilege of his friendship. The work was partially supported by the Italian ASI Agency under Contract No. I/R/214/02.

References and Notes

(1) Lahee, A. M.; Toennies, J. P.; Wöll, Ch. *Surf. Sci.* **1986**, *177*, 371.
(2) Froitzheim, H.; Schulze, M. *Surf. Sci.* **1989**, *211/212*, 837.
(3) Ogletree, D. F.; Van Hove, M. A.; Somorjai, G. A. *Surf. Sci.* **1986**, *173*, 351.
(4) Baro, A. M.; Ibach, H. *J. Chem. Phys.* **1979**, *71*, 4812.
(5) Malik, I. J.; Trenary, M. *Surf. Sci.* **1989**, *214*, L237.
(6) Olsen, C. W.; Masel, R. I. *Surf. Sci.* **1988**, *201*, 444.
(7) Segner, J.; Campbell, C. T.; Doyen, G.; Ertl, G. *Surf. Sci.* **1984**, *138*, 505.
(8) Hoge, D.; Tüshaus, M.; Schweizer, E.; Bradshaw, A. M. *Chem. Phys. Lett.* **1988**, *151*, 230.
(9) Yeo, Y.Y.; Vattuone, L.;King, D. A. *J. Chem. Phys.* **1997**, *106*, 392.
(10) Tully, J. C. *J. Chem. Phys.* **1980**, *73*, 6333.
(11) Billing, G. D. *Chem. Phys.* **1984**, *86*, 349.
(12) Billing G. D.; Cacciatore, M. *Chem. Phys. Lett.* **1985**, *113*, 23.
(13) Billing, G. D.; Cacciatore, M. *Chem. Phys.* **1986**, *103*, 137.
(14) Völkening, S.; Wintterlin, J. *J. Chem. Phys.* **2001**, *114*, 6382.
(15) Harris, J. In *Dynamics of gas−surface interactions*; Rettner, C. T., Ashfold, M. N. R., Eds.; The Royal Society of Chemistry: Cambridge, U.K., 1991.
(16) Billing, G. D. *Chem. Phys.* **1982**, *70*, 223.
(17) Billing, G. D. *Chem. Phys.* **1983**, *74*, 143.
(18) Gross, A.; Wilke, S.; Scheffler, M. *Phys. Rev. Lett.* **1995**, *75*, 2718.
(19) Gundersen, K.; Hammer, B.; Jacobsen, K. W.; Nørskov, J. K.; Lin, J. S.; Milman, V. *Surf. Sci.* **1993**, *285*, 27.
(20) Blyholder, G. *J. Phys. Chem.* **1964**, *68*, 2772.
(21) Ge, Q.; Hu, P.; King, D. A.; Lee, M. H.; White, J. A.; Payne, M. C. *J. Chem. Phys.* **1997**, *106*, 1210.
(22) Hu, P.; King, D. A.; Lee, M. H.; Payne, M. C. *Chem. Phys. Lett.* **1995**, *246*, 73.
(23) Philipsen, P. H. T.; te Velde, G.; Baerends, E. J. *Chem. Phys. Lett.* **1994**, *226*, 583.
(24) Morikawa, Y.; Mortensen, J. J.; Hammer, B.; Nørskov, J. K. *Surf. Sci.* **1997**, *386*, 67.
(25) Hammer, B.; Morikawa, Y.;Nørskov, J. K. *Phys. Rev. Lett.* **1996**, *76*, 2141.
(26) Curulla, D.; Clotet, A.; Ricart, J. M.; Illas, F. *J. Phys. Chem. B* **1999**, *103*, 5246.
(27) Liu, Z. P.; Hu, P. *J. Chem. Phys.* **2001**, *114*, 8244.
(28) Herzberg, G. Molecular Spectra and Molecular Structure I. *Spectra of diatomic molecules*; Van Nostrand: Princeton, NJ, 1950.
(29) Cacciatore, M.; Billing, G. D. *Surf. Sci.* **1990**, *232*, 35.
(30) Billing, G. D. *J. Phys. Chem.* **1995**, *99*, 15378.
(31) Henriksen, N. E.; Hansen, F. Y.; Billing, G. D. *Chem. Phys. Lett.* **1995**, *244*, 350.
(32) Billing, G. D.; Guldberg, A.; Henriksen, N. E.; Hansen, F. Y. *Chem. Phys.* **1990**, *147*, 1.
(33) Wang, L.;Billing, G. D. *Chem. Phys.* **1997**, *224*, 65.
(34) Billing, G. D. *J. Phys. Chem.* **2001**, *105*, 2340.
(35) Billing, G. D. *Comput. Phys. Rep.* **1990**, *12*, 383.
(36) Billing, G. D. *Dynamics of Molecule Surface Interactions*; Wiley: New York, 2000.
(37) Iannotta, S.; Gravili, C.; Boschetti, A.; Cagol, A.; Cacciatore, M. *Chem. Phys.* **1995**, *194*, 133.